The role of temperature and carbon dioxide climatic stress factors on the growth kinetics of *Escherichia coli*

[1] Styliani Roufou, [1,3] Sholeem Griffin, [1]Juan Attard, [2] Lydia Katsini, [2] Monika Polańska , [2] Jan F.M. Van Impe, [4] Ruben Gatt and, [1,3,5] Vasilis P. Valdramidis*

[1] University of Malta, Faculty of Health Sciences, Department of Food Sciences and Nutrition, MSD2080, Malta

[2] KU Leuven, Department of Chemical Engineering BioTeC+, Chemical & Biochemical Process Technology & Control Chemical, Ghent 9000, Belgium

[3] University of Malta, Centre of Molecular Medicine and Biobanking, MSD2080, Malta

[4] University of Malta, Faculty of Science, Department of Metamaterials Unit, MSD2080, Malta

[5] National Kapodistrian University of Athens, School of Science, Department of Chemistry, 157 71 Athens, Greece

Corresponding author

E-mail: vasilis.valdramidis@um.edu.mt; vasilis.valdramidis@chem.uoa.gr

Address: University of Athens, Faculty of Science, Department of Chemistry, Athens, Greece

Abstract

Aims

The global level of carbon dioxide and temperature in the atmosphere is expected to increase, which may affect the survival of the stress-adapted bacteria. In this study, the effect of temperature and dissolved carbon dioxide on the growth rate of *Escherichia coli* was studied, thus assessing its response to induced environmental stress factors.

Methods and Results

A kinetic assay has been performed using a microplate reader with a spectrofluorometer to determine the specific growth rates. Polynomial models were developed to correlate the environmental conditions of *temperature* and *carbon dioxide* with *E. coli* BL21 (DE3) growth in culture media and dairy by-products. At a temperature of 42°C, as the dissolved CO_2 increased, a

decrease of the μ_{max} by 0.76 h^{-1} was observed. In contrast, at 27°C, this increase led to a rise of the μ_{max} by 0.99 h^{-1}. Moreover, a correction factor was added when applying the model to dairy whey samples.

Conclusions

The application of this developed model can be considered a useful tool for predicting the growth of *E. coli* using climate projections.

Significance and Impact of Study

This is the first study to develop a predictive model for the growth of *Escherichia coli* using the climatic parameters of temperature and carbon dioxide.

Keywords

Stress-adapted bacteria, fluorescence readings, predictive microbiology, climate change, growth kinetics

Introduction

Climate change is associated with extreme weather phenomena like heatwaves or extended windy-rainy periods. Changes in global weather are expected to affect agriculture practices (Roufou et al., 2021). The impact of climate change on food production can be multifold. It can directly affect the animals themselves, causing animal stress and changes in milk composition and indirectly adverse changes to crop cultivation by an aggravated exposure to resistant parasites and pathogens. Between 1880 and 2018, the global atmospheric temperature increased by 1°C (IPCC, 2019). According to estimates by DTE (2021), an annual increase of 2.50 ppm in atmospheric carbon dioxide (CO_2) will make 2021 the first year, with an annual average of CO_2 50% above its pre-industrial levels. More specifically, atmospheric carbon dioxide was around 417.30 ppm by the end of 2021. The continuous rise of atmospheric CO_2, combined with the reaction of dissolved CO_2 (DCO_2) with water, forming carbonic acid (H_2CO_3), is expected to cause a decrease of 0.30 - 0.40 in the pH of seawater by the end of this century. Therefore, it could affect the survival of animals, microbiota and plants (Huang et al., 2018, Roufou et al., 2021).

Climate change has also been recognised as having a potential effect on the increase of the bacterial contamination of food, waste and water, which in turn may lead to a change in the risks associated

with water and foodborne infection diseases (Miraglia et al., 2009). Critical factors, like nutrients, temperature and CO_2, are known to affect microbial proliferation, although not all microorganisms are sensitive to the effect of CO_2 (Oliveira et al., 2010). Some stress-adapted bacteria, such as *Listeria* (*L*.) spp. and *E. coli*, have been reported to passively diffuse CO_2 from the cytoplasm into the cell, biosynthesizing various small molecules such as pyrimidines. Therefore, CO_2 could also enhance their growth and lead to a critical public health problem, such as the spread of diseases, under climatic forecasts (Zhu et al., 2015, Merlin et al., 2003). Further analysis of the microbial growth kinetics under increased CO_2 and temperature conditions is required in order to assess any potential human health and food safety risks associated with bacterial infections.

Listeria spp. and *E. coli* are foodborne microbes with low infectious doses, which can cause severe illness (Kanda et al., 2020). Their ability to survive and thrive under thermal shock and acid stress is critical for their successful transmittance to humans (Arcari et al., 2020). The study of Koutsoumanis and Sofos (2004) concluded that *E. coli* O157:H7 has a more efficient acid resistance system than *L. monocytogenes*. It also has a remarkable and well-studied ability to withstand exposure to exceptional conditions and activate responses at the gene expression level. Furthermore, the anaerobic metabolic abilities of *E. coli* have been used to overcome the electrochemical reactions in the presence of oxygen, which cause the production of bactericidal compounds such as hydrogen peroxide (Tashiro et al., 2018). It is also known that an induced autotrophic *E. coli* BW25113 strain can utilise metabolic pathways already optimised to produce fuels and chemicals from CO_2 (Kruyer and Peralta-Yahya, 2020). The short production time (usually eight - 10 generations per day) and the small genome (5 M bases) make it a valuable model for assessing induced stress responses (Wang et al., 2018).

E. coli overcome temperature changes and high CO_2 levels, as reported in studies of food products under Modified Atmosphere Packaging (MAP) conditions. Song et al. (2019) concluded that in spinach packaging, the increase of CO_2 concentration from 3 to 15% v/v at 15^{o}C facilitated the microbial growth of *E. coli* O157:H7 due to its escape from oxidative stress. Sharma et al. (2011) studied the *E. coli* O157:H7 responses when contaminated on iceberg lettuce in MAP. They stored the samples at 15^{o}C, with oxygen (O_2) and CO_2 ranging from 0 to 1.5% v/v and 0.5 to 8.9% v/v, respectively. They concluded that *E. coli* O157:H7 grew was promoted by 0.26 $\log_{10}$ CFU g^{-1} under atmospheric O_2 and 0.37% v/v CO_2 compared to the other conditions. The same strain of *E. coli* was

reported to survive when stored at 5 and 25^{o}C under MAP conditions of 8 % v/v and 13.3% v/v of CO_2, respectively (Boz et al., 2018, Oliveira et al., 2010).

In addition to the foods mentioned above, *E. coli E. coli* has also been identified as one of the main etiologies among the bacteria associated with bovine mastitis, and it is prevalent in the dairy industry (Bag et al., 2021). Therefore, in whey samples, *E. coli* was found to be the fourth most abundant species during the winter months (da Silva Duarte et al., 2020). Currently, the dairy sector is generated over 190 million tons of whey annually, which is a significant environmental issue due to the massive volumes and organic content of this by-product (Yadav et al., 2015). Hence, the number of microbes, such as *E. coli,* dumped into the environment is vast. These microbes are exposed to environmental conditions which are affected by the climate change phenomenon. Consequently, it is imperative to understand how *E. coli* responds to stress at high temperatures and CO_2 levels, which exceed previous MAP studies and are more representative of climate stress conditions. This will allow the development of new, more accurate risk assessment studies in the area of food safety.

There are many methods to quantify the responses of *E. coli* under different stressing conditions; in particular, fluorescence can easily be used for live/dead kinetics experiments due to its accurate readings and better selectivity than other techniques (Rajapaksha et al., 2019). Green fluorescent protein (GFP) has been used as a reporter gene for the assessment of viability. Genetically modified *E.coli* with the *gfp* gene produces the GFP protein, which fluoresces when excited with UV light at 396nm. The GFP protein is synthesised in transformed cells, which tags them and remains fluorescence as long as the protein is retained (Lowder et al., 2000). Enhanced GFP (eGFP) was developed to increase fluorescence efficiency and improve its expression in prokaryotic and eukaryotic systems (Ganini et al., 2017). The expression of recombinant proteins in *E. coli* can be accomplished by inserting a gene into a plasmid vector under the transcriptional control of a promoter (Gomes et al., 2020). This can make *E. coli* an ideal microbial model for monitoring microbial responses under stress conditions.

The current study developed a method to estimate the DCO_2 in aqueous solutions. In addition, an *E. coli* BL21 (DE3) strain expressing the eGFP protein was used as a target strain to assess its growth kinetics under different temperatures and CO_2-induced climatic stress conditions. The developed

model was validated with an independent data set and was then applied to determine the growth of *E. coli* in sterile whey samples under similar conditions.

Materials and methods

Preparation of culture media and food matrices

Miller's Lysogeny Broth (LB) was produced with 10 g L^{-1} tryptone (Biochem, France), 5 g L^{-1} bacto yeast extract (BD, Belgium), and 10 g L^{-1} NaCl (Fisher Scientific, United Kingdom); while the pH was adjusted, with pH meter (3520, Jenway), at 7 ± 0.2 with 1 mol L^{-1} NaOH solution. An additional 15 g L^{-1} agar (Biolab, Hungary) was added before pH adjustment to produce LB agar when indicated. The solution was then autoclaved at 121°C for 15 min (Rodwell Phoenix 60 MP25, England). Prior to the addition of ampicillin solution (HiMedia, India) at the concentration of 0.29 mmol L^{-1}, the mixture was cooled to 50°C in a water bath. Approximately 20 mL of the mixture was dispensed into petri dishes and allowed to cool to form agar plates, which were then stored at 4°C.

Whey samples used in this study were prepared using commercial pasteurized low-fat bovine milk at room temperature and adding microbial rennet (Fromase 220 IMCU, DSM, France). The solution was mixed and placed in a water bath at 37°C for 45 min to coagulate the casein. The cheese was then cut into pieces and remained in the water bath for another 15 min. Finally, the whey was separated by filtration with one layer of cotton gauze, and it was then filter sterilized with a 0.22µm vacuum filtration system (Stericup, Germany). The pH of the whey sample was 6.76 at 37°C.

Generation of an eGFP-tagged *E. coli* clone

A plasmid coding for the production of eGFP was required to produce an eGFP-producing bacterial clone with pAP1698-4 (Addgene, United States, Code n°105242) as the donor plasmid. The donor plasmid was cloned into *E. coli* DH5α (Thermofisher, United States) by mixing 10 ng of plasmid DNA with the *E. coli* DH5α cells. This was followed by 30 min incubation on ice, a heat shock for 30 s at 42°C in a water bath (Grant TXF200, United Kingdom) and a 2 min recovery on ice. Then, 950 µL of Super Optimal broth with Catabolite repression (SOC) outgrowth media (New England Biolabs, United Kindgom) was added to the microcentrifuge tubes, which were then incubated for 1 h at 37°C, rotating at 225 rpm. Aliquots of 20, 100, and 200 µL were then placed onto selective LB plates containing 100 µg mL^{-1} ampicillin. Colonies visible after 16-24 h incubation at 37°C were then used

to create overnight cultures: 50 mL conical centrifuge tubes filled with 10 mL LB-ampicillin were inoculated using single colonies and left incubating at 37°C at 200 rpm for 16-24 h overnight.

For insertion into the recipient plasmid pD454-MBP (T7-MBP-ORF, Ecoli-ElecD, ATUM Bio, United States), extraction of pAP1698-4 from *E. coli* DH5α was done using the ZR Plasmid Miniprep^{TM}-Classic kit (D4015, Zymo Research, United States) according to the manufacturer's instructions. eGFP gene was amplified using specific PCR primers from the pAP1698-4 plasmid, which resulted in a 720 bp fragment. Gel electrophoresis was performed using a 100 bp ladder, purified PCR product (741 bp), and the donor plasmid pAP1698-4 (3404 bp), which verified the correct product size. Purification of the eGFP PCR product was done using the NucleoSpin ® Gel and PCR Clean-up kit as per the manufacturer's instructions (Machery-Nagel, Germany). The recipient plasmid pD454-MBP contains overhangs and thus, the gene insert must have compatible overhangs for successful ligation of the eGFP PCR product. The restriction enzyme SapI was used to obtain compatible overhangs by 1 µL PCR product to make a 20 µL reaction mix as per the manufacturer's guidelines (New England Biolabs, United Kingdom). The Bio-Rad T100 TM Thermal Cycler was used to incubate the mixture at 37°C for 16 h, followed by a 20 min incubation at 65^{o}C for thermal inactivation of the enzyme, then maintained at 12°C until removed.

The mix was then purified using the NucleoSpin ® Gel and PCR Clean-up kit (Machery-Nagel, Germany). The compatible DNA overhangs obtained via digestion of the eGFP PCR product and available in the ready-to-use linearised pD454-MBP backbone were ligated using T4 DNA ligase using manufacturer's guidelines by preparing a ligation mix that was incubated at 16°C for 16 h (New England Biolabs, United Kingdom). The NEBioCalculator was employed to determine the necessary volumes and ratios to be used based on the size of the insert (720 bp + overhangs) and the vector (5122 bp + overhangs).

As previously described, the assembled pD454-MBPeGFP plasmid was transformed in *E. coli* DH5α by the chemical transformation method and stored at -80°C in 20% glycerol-LB to maintain a high-copy number. The pD454-MBPeGFP plasmid was extracted from *E. coli* DH5-α using the ZR Plasmid Miniprep^{TM}-Classic kit and transformed into *E. coli* BL21 (DE3) by chemical transformation as previously described (New England Biolabs, United Kingdom). The successful transformation procedure of restriction and ligation of the PCR product was confirmed and demonstrated by the growth of white colonies in the presence of X-Gal (Thermofisher, United States) Isopropyl-1-thio-β-

D-galactopyranoside (IPTG) solution (ThermoFisher, Lithuania) and ampicillin, using the *lac operon* for screening. Colonies were checked for light emission using the OLYMPUS BX63 U-RFL-T microscope with immersion oil Type FF (BioGnost, Croatia, Ref IUF-30). Lastly, the function of pD454-MBPeGFP in the presence of ampicillin was determined according to the growth curves generated from a viable plate counting method. For *E. coli* BL21 (DE3), a fresh culture (37°C, 18 h) was used to inoculate 100 mL of LB broth at Log_{10} 2 CFU mL^{-1}. Aliquots were taken after 0, 2, 4, 6, 8, 10, 12, 14, 16, and 18 h of incubation, and 100µL was plated out in duplicate on LB agar. Following an 18-24 h incubation at 37°C, the CFU number was recorded, and thus the Log_{10} CFU mL^{-1} was determined. An identical procedure was run in parallel for *E. coli* BL21 (DE3) pD454-MBPeGFP (*E. coli* pD454-MBPeGFP), using LB-ampicillin instead. This experiment was performed in triplicate.

E. coli pD454-MBPeGFP sub-culture conditions

The stock strain was maintained at -80°C in cryovials in a final concentration of 20% glycerol (Honeywell, Malaysia) Lysogeny Broth solution. The stock *E. coli* pD454-MBPeGFP strain was streaked on LB-ampicillin agar plates (37°C, 18 h) and stored at 4°C for a short time before use. For the overnight cultures, three colonies from the plate were inoculated in 10 mL LB-ampicillin broth at 37°C, shaking at 220 rpm for 18 h. The overnight cultures were washed with 10 mL of LB broth using a centrifuge at 6461 x g for 5 min. The supernatant was decanted, and the pellet was resuspended in 10 mL LB broth when the analysis was held for the LB broth and 10 mL of Ringer's sterile solution for the whey samples. Cells were harvested by transferring 210 µL of the cell suspension to microcentrifuge tubes and centrifuged at 11,000 x g for 2 min. The final cell pellet was resuspended in fresh 1 mL LB-ampicillin-IPTG, 0.42 µM IPTG when the analysis was held for the LB broth and 1 mL of whey-ampicillin-IPTG samples in order to get 10^8 CFU mL^{-1}. Washed cultures were 10-fold diluted in LB-ampicillin-IPTG broth and whey-ampicillin-IPTG, respectively, to produce a starting concentration of ~10^6 CFU mL^{-1}, and 360 µl of this was transferred to the first column of a sterile 96-well black plate (Thermo Scientific, United States, 96F NonTreated Black Microwells). Based on the set-up, the remaining plate was then filled up with LB-ampicillin-IPTG broth or whey-ampicillin-IPTG. A two-fold serial dilution of the inoculum was performed, resulting in 180 µL per well.

227 Determination of the specific growth rates of *E. coli* pD454-MBPeGFP strain in LB-/ whey-
228 ampicillin-IPTG broth by fluorescence measurements
229 The effect of temperature and CO_2 on the maximum specific growth rate (μ_{max}) of the *E. coli*
230 pD454-MBPeGFP strain was assessed in the previously produced LB-ampicillin-IPTG broth having pH
231 at 7 ± 0.02. In order to assess a wide growth range associated with the future global climatic
232 projections (IPCC, 2019) and limitations of the device, six different temperatures, 27, 30, 34, 37, 40,
233 and 42°C, and seven different CO_2 levels ranging from 0.2, 1, 2.5, 4, 6, 8, and 10% v/v in air, as
234 defined by the manufacturer, were studied in a microplate fluorospectrometer (Tecan Spark 10M,
235 Switzerland). The whey-ampicillin-IPTG samples were tested at three different temperatures of 27,
236 34 and 42°C, and CO_2 levels ranging from 0.2, 0.5 and 1% v/v in air. These conditions correspond to
237 future climatic projections in which this by-product is exposed. Fluorescence signals were measured
238 automatically every 10 minutes at the target conditions for 24 hours using a microplate reader.
239 Shaking method at 216 rpm was applied for 10 sec prior to every reading in the microplate reader.
240 The Excitation/Emission (Ex/Em) wavelengths were set for eGFP at 485/510 nm. Seven different
241 gains (45, 50, 55, 60, 65, 70, and 75) were measured at 485/510 nm to ensure an optimal signal-to-
242 noise ratio. The percentage error of the fluorescence readings from the three different inoculum
243 sizes was studied to optimise the gain. Each point was generated from the average of two biological
244 replicates.
245
246 The μ_{max} was determined using the fluorescence growth curves. The method of Cuppers and Smelt
247 (1993) and Membre et al. (2002) was considered for the calculations. In this method, the μ_{max} was
248 computed by the logarithmic phase based on the principle of binary fission. The time taken by the
249 bacteria to double in number during a specified time is known as the generation time (g_{time}), and
250 the population levels can be defined as follows:
251 $$N_t = N_0 \times 2^n \quad (1)$$
252 where N_t is the population at time t [CFU mL^{-1}], N_o is the initial population number [CFU mL^{-1}], and
253 n is the generation number. Considering that the rate of increase of N_t with time is just proportional
254 to the number of cells present at any moment in time; equation (1) can be re-written as
255 $$\mu_{max} \times t = n \times ln2 \quad (2)$$
256 or
257 $$\mu_{max} = \frac{ln2}{g_{time}} \quad (3)$$

where μ_{max} at [h^{-1}]. Hence, the g_{time} can be computed for every dilution value from the fluorescence reading [RFU]. Binary dilutions were analysed from the microtiter plate to estimate the μ_{max}; hence, the range of initial concentrations examined was approximately 10^6 - 10^4 CFU mL^{-1}.

Measuring the DCO_2 in the LB-ampicillin-IPTG broth and whey sample

The amount of DCO_2 present in the nutrient broth (LB-ampicillin-IPTG and whey-ampicillin-IPTG in the case of this study) depends on environmental conditions such as temperature and atmospheric CO_2. In view of this, a method to estimate the amount of DCO_2 in the nutrient broth at different temperatures and atmospheric CO_2 concentrations was developed. This method is based on the knowledge that the dissolution of CO_2 has an effect on the pH of the broth, whereby the higher the amount of DCO_2, the lower the pH. This relation stems from the reaction of CO_2 with water to form carbonic acid, which may then dissociate to form hydrogen carbonate and carbonate ions (see eq. 4 to 6) (Millero et al., 2006).

$$H_2O + CO_2 \underset{\rightleftharpoons}{K_0} H_2CO_3 \qquad K_0 = \frac{[H_2CO_3]}{[CO_2]} \tag{4}$$

$$H_2CO_3 \underset{\rightleftharpoons}{K_1} H^+ + HCO_3^- \qquad K_1 = \frac{[HCO_3^-]\times[H^+]}{[H_2CO_3]} \tag{5}$$

$$HCO_3^- \underset{\rightleftharpoons}{K_2} H^+ + CO_3^{2-} \qquad K_2 = \frac{[CO_3^{2-}]\times[H^+]}{[HCO_3^-]} \tag{6}$$

If the nutrient broth is maintained at a pH lower than 8.3, one may assume that the hydrogen carbonate does not dissociate to the carbonate (Stumm and Morgan, 1996). In this case, the concentration of DCO_2 may be given by:

$$[CO_2] = \frac{[H_2CO_3]}{K_0} \tag{7}$$

where

$$[H_2CO_3] = \frac{[HCO_3^-]\times[H^+]}{K_1} \tag{8}$$

Note that K_1 and K_0 are the dissociation constants for carbonic acid and carbon dioxide, respectively (for the calculation of K_0 and K_1, refer to Roufou et al. (2022)).

Due to the nature of this study, a spectrophotometric method was developed to assess the pH and hence the amount of DCO_2. For this purpose, two pH indicators were utilised, phenol red (Fisher Scientific, United Kingdom) and methyl red (LabPaK, United Kingdom). The use of methyl red was only used for the LB-ampicillin-IPTG samples due to the pH of the solution. Phenol red (PR) has a pH sensitivity ranging from 8.2 to 6.2 (Held, 2018), while for methyl red (MR) ranges between 6.3 to 4.4 (Zhang et al., 2012) (for more details on the preparation of the solutions, refer to (Roufou et al.,

2022)). Both of these indicators are weak acids, with the acidic HI^- and basic I^{2-} forms of the indicators having a maximum absorption at a wavelength of λ_1 and λ_2, respectively. The ratio of the maximum spectrophotometric absorbance of the basic and acidic forms (R) can be used to estimate the pH as (Lai et al., 2016, Yao and Byrne, 2001):

$$pH = -log[H^+] = pK_I + log\frac{(R-e_1)}{(e_2-R\times e_3)} \quad (9)$$

where pK_I is the dissociation constant of the indicator. The term $\frac{(R-e_1)}{(e_2-Re_3)}$ is equal to the ratio of $[I^{2-}]$ and $[HI^-]$, with e_1, e_2, and e_3 refering to the molar absorption coefficient ratios, which may be defined as:

$$e_1 = \frac{\varepsilon_{HI,A_2}}{\varepsilon_{HI,A_1}}\ ,\ e_2 = \frac{\varepsilon_{I,A_2}}{\varepsilon_{HI,A_1}}\ ,\ e_3 = \frac{\varepsilon_{I,A_1}}{\varepsilon_{HI,A_1}} \quad (10)$$

where $\varepsilon_{HI,A1}$, $\varepsilon_{HI,A2}$, are expressed as the absorbance of the acidic form at the two wavelengths, respectively, divided by the indicator concentration and path length (l), and the $\varepsilon_{I,A1}$, $\varepsilon_{I,A2}$ are expressed in terms of absorbances in the basic form, with the indicator concentration, and l (for the estimation of e_1, e_2, and e_3, please refer to Roufou et al. (2022)).

At this point, one must also take into consideration that the presence of the indicator (PR or MR) may have a significant influence on the pH of the nutrient broth, particularly at relatively low atmospheric CO_2 concentrations. In addition, the LB broth is prepared with the addition of sodium chloride. To account for these factors, equation 8 was modified to:

$$[H_2CO_3] = \frac{(2\times[H^+]\times[HCO_3^-])^2 - [HCO_3^-]^2 - (4\times K_I\times[IND])}{4\times K_1} \quad (11)$$

where, K_I is the dissociation constant of the indicator and [*IND*] is the concentration of the indicator.

Experimentally, the effect of temperature and atmospheric CO_2 on DCO_2 was analysed by filling a 96-well transparent plate (Thermo Scientific, United States, 96F NonTreated Transparent Microwells) with 180 µL of LB-ampicillin-IPTG solution. In each case, the temperatures and atmospheric CO_2 was set to vary as described in section 2.2, *i.e.* from 0.2 to 10% v/v in the case of atmospheric CO_2 and from 27 to 42°C in the case of temperature (Roufou et al., 2022). During the experiment, the absorbance for samples having the PR indicator was measured at A_1= 430 nm and A_2= 558 nm, while the absorbance for the samples having MR as an indicator was measured at A_1= 526 nm and A_2= 434 nm.

Model development

In order to describe the μ_{max} as a function of the temperature and DCO_2, two polynomials structures have been considered. The general second-order and third-order response surface models with interaction factors were expressed as follows:

$$\mu_{max} = b_0 + b_1 \times T + b_2 \times DCO_2 + b_3 \times T \times DCO_2 + b_4 \times T^2 + b_5 \times DCO_2^2 \quad (12)$$

$$\mu_{max} = b_0 + b_1 \times T + b_2 \times DCO_2 + b_3 \times T^2 + b_4 \times DCO_2^2 + b_5 \times T^2 \times DCO_2 + b_6 \times T \times DCO_2^2 + b_7 \times T^3 + b_8 \times DCO_2^3 \quad (13)$$

where b_i are the polynomial coefficients and T and DCO_2 are the temperature [°C] and DCO_2 [ppm], respectively. The *partial F-test* (a= 0.99) was used for eliminating non-significant terms.

The fitting capacity was assessed based on the Root Mean Squared Error, *RMSE*, and the coefficient of determination (R^2).

$$RMSE = \sqrt{\frac{\sum_{i=1}^{n_t}(Y_{exp} - Y_i)^2}{n_t - n_p}} \quad (14)$$

$$R^2 = 1 - \frac{SSE}{SST} = 1 - \frac{\sum_{i=0}^{N}(Y_i - Y_{exp})^2}{\sum_{i=0}^{N}(Y_{mean} - Y_{exp})^2} \quad (15)$$

where Y_i represents the predicted value of the dependent variable by the regression model, Y_{exp} is the experimental data, n_t is the total number of data points, n_p is the number of estimated model parameters, N represents the number of predicted values, and Y_{mean} is the mean of the predicted value (Akhlaghi et al., 2019, Valdramidis et al., 2010).

The dataset was randomly split into two datasets– the training dataset for the development of the prediction model (70%) and the validation dataset for the validation of the model (30%). The performance of the developed models was evaluated by estimating the bias (B_f) and accuracy (A_f) factors as proposed by Ross (1996):

$$B_f = 10^{\left(\frac{\sum_{i=1}^{n} log_{10}(pd_i/ob_i)}{n}\right)} \quad (16)$$

$$A_f = 10^{\left(\frac{\left|\sum_{i=1}^{n} \log_{10}(pd_i/ob_i)\right|}{n}\right)} \quad (17)$$

where pd_i is the population level predicted by the model, ob_i is the observed population level, and n is the number of observations. Moreover, the effectiveness of the developed model to predict the growth of *E. coli* on food by-product was tested, and the addition of correction factor, i, was added

to the final model corresponding to the nutrient differences between culture medium and food matrices.

Statistical analysis and software programs

The software Graphpad Prism 8.0.1 was used to perform normality tests and a Two-way ANOVA for the obtained μ_{max} with P <0.0001. The final +/- error of the DCO_2 was calculated based on the uncertainty propagation method as described by (Bevington and Robinson, 2003). The correction factor was estimated in Microsoft Excel (version 2019). For simulation, statistical analysis (such as *F-test*, determination of R^2), fitting of the model, and the programming code was written in MATLAB (Version 2020b), and lsqnonlin solver was used (The MathWorks, Natick, USA).

Results

The current study aimed to assess the effect of the induced environmental stress factors of temperature and DCO_2 on the growth of *E. coli*. This was achieved firstly by producing the *E. coli* eGFP strain, then optimising the sensitivity of the fluorescence gain of the device in order to detect *E. coli* pD454-MBPeGFP growth as a function of eGFP reporter protein expression and minimising the background noise. Secondly, a method for estimating the DCO_2 in the LB-Amp-IPTG broth and dairy by-product was optimised under different environmental conditions, and the growth responses of *E. coli* pD454-MBPeGFP were quantitatively assessed. This allowed an understanding of the interaction between the environmental conditions and *E. coli* pD454-MBPeGFP via a response surface model.

Creation of eGFP-tagged *E. coli* strains

The function of the pD454-MBPeGFP was confirmed by observing no blue colonies at the X-Gal, IPTG and ampicillin analysis, showing a lack of recipient plasmid pD454-MBP self-ligation. When growing onto LB-ampicillin-IPTG agar and viewed using fluorescent imaging techniques (Fig 1a), the eGFP-tagged strain emitted green light. Furthermore, the results of viable plate counts of *E. coli* BL21 (DE3) and *E. coli* pD454-MBPeGFP are shown in (Fig 1b). Readings for the first six hours were below the detection limit of 1.3. An increased lag phase for *E. coli* pD454-MBPeGFP compared to *E. coli* BL21 (DE3) is evident as the inflexion point appears later. Moreover, the presence of high error bars from the plate counting in some temperatures for both strains highlighted the need for an alternative, more accurate measuring method.

Assessing the microbial growth

This study first optimised a system for determining the microbial growth of *E. coli* pD454-MBPeGFP in culture media. The gain optimising analysis has shown that offsetting the gain to 50 gave an average percentage error of about 10% RFU (Fig 2). The optimal gain adapted during the kinetic measurements can be different from the actual optimal gain because there is a non-linear relationship between the gain and the fluorescence signal. The fluorescence signal will increase over time, and the optimal gain may reach saturation (Engelbrecht et al., 2009). Furthermore, since the concentration of eGFP being expressed cannot be altered and is a product of growth; therefore, the gain was adjusted to allow for the complete growth curve to be recorded with the highest sensitivity at the low fluorescence signal during the lag phase without saturation at high fluorescence signal during the stationary phase of growth. Overall, the gain is a parameter which characterized the fluorescent capacity of *E. coli* pD454-MBPeGFP; hence in this study, the same gain was used for the whey-ampicillin-IPTG set-up.

Using the fluorescence readings, the effect of temperature (range: 27 - 42^{o}C) and CO_2 (range: 0.1 – 10% v/v in the air) on the growth of *E. coli* pD454-MBPeGFP was studied. The raw fluorescence curves with the calculated g_{time} are presented in (Fig 3a) at 40^{o}C and 0.2% v/v CO_2 in the LB-ampicillin-IPTG broth. The g_{time} of the three biological replicates was plotted against the generation number. In Fig 3b, the result from the linear regression of the growth of *E. coli* pD454-MBPeGFP at the same conditions is presented. The ratio of the *ln2* with the linear regression slope determined the μ_{max} values as described in section 2.2. A Two-way ANOVA and normality tests of Anderson-Darling and Kolmogorov-Smirnov were applied by using the temperature and levels of CO_2. The analysis showed that the results were normally distributed. Additionally, from Fig 4 the μ_{max} at a high temperature of 42^{o}C and low level of CO_2 0.2% v/v was significantly higher than that reported at a low-temperature 27^{o}C and high level of CO_2 6% v/v (*P <0.0001*). As the temperature increased from 27 to 42^{o}C, at the CO_2 level of 0.2% v/v, the μ_{max} was increased by 1.07 h^{-1}. In contrast, the reverse phenomenon occurred when the DCO_2 increased from 0.2 to 10% v/v in the temperature from 37 to 42^{o}C.

Estimation of the dissolved CO_2 (ppm) in the LB- /whey-ampicillin-IPTG samples.

The DCO_2 in the LB-ampicillin-IPTG broth was used for the microbial modelling analysis. When the percentage of CO_2 in the system increased, the DCO_2 increased proportionally. Furthermore, the DCO_2 decreased as the temperature increased, following Henry's law. Similarly to culture media,

412 the whey sample followed Henry's law (Fig 5). The study of Adnan et al. (2020) concluded that
413 temperature is characterised as the most significant parameter for CO_2 absorption in culture media
414 solutions, with *P <0.0001*. Moreover, solutions of different compositions can cause differences in
415 the amount of DCO_2. In this study, the DCO_2 obtained by flowing 2% v/v CO_2 in the system at
416 temperatures 27 and 40°C resulted in 222 ppm and 104 ppm of DCO_2, respectively (Fig 5a).
417 Moreover, the whey-ampicillin-IPTG sample has less salt concentration than LB-ampicillin-IPTG,
418 resulting in more DCO_2 under the same conditions than the broth (Fig 5b). In this study, the DCO_2 in
419 the whey samples obtained by flowing 10% v/v CO_2 in the system at temperatures 27 and 42°C
420 resulted in 2176 ppm and 1973 ppm in DCO_2, respectively.
421

422 ## Development of a secondary microbial model

423 Cardinal values type or other secondary models have a model structure that assumes that multiple
424 inhibitors are combined independently and cannot be used for different systems. From the Two-way
425 ANOVA, it can be concluded that there is a synergistic effect of DCO_2 for different temperatures on
426 the growth of *E. coli* pD454-MBPeGFP. Hence, polynomial equations were derived for correlating
427 the estimated μ_{max} with the DCO_2 in the medium and different temperatures. In order to develop
428 the models, 29 random conditions were used as a training dataset, while 11 were for validation. The
429 selected datasets for training and validation are represented in Fig 4. The analyses of the *partial F-*
430 *test* concluded that not all the parameters appeared to be significant (Tables 1 and 2). More
431 specifically, the parameters which supported the Null Hypothesis have been excluded (Glen, 2021).
432 After eliminating the non-significant parameters, the models of the μ_{max} are expressed as follows :

433 $$\mu_{max} = -8.23 + 0.42 \times T + 0.01 \times DCO_2 - 2.77 \times 10^{-4} \times T \times DCO_2 - 4.56 \times 10^{-3} \times T^2 \quad (18)$$

434 $$\mu_{max} = 29.40 - 2.87 \times T + 4.72 \times 10^{-3} \times DCO_2 + 0.09 \times T^2 - 3.91 \times 10^{-6} \times T^2 \times DCO_2 -$$
435 $$9.00 \times 10^{-4} \times T^3 \quad (19)$$
436

437 The developed secondary model Eq. (18) gave a fitting capacity of R^2 = 0.74, *RMSE* = 0.17, and the
438 saddle point of this model is at 34°C and 381 ppm DCO_2. While the third-order polynomial model,
439 Eq. (19), gave a fitting capacity of R^2 = 0.80, *RMSE* = 0.15 and a saddle point at 35°C and 517 ppm.
440 In addition to the fitting capacity, the validity of the developed models was further evaluated
441 through the estimation of B_f and A_f using the validation dataset (11 conditions). The B_f and A_f for
442 model Eq. (18) were 0.85 and 1.74, respectively, while for model Eq. (19) were 1.13 and 1.30,
443 respectively. Comparing the fitting capacity and the B_f and A_f factors of the developed models Eq.
444 18 and 19, the latter Eq. (19) demonstrated satisfactory performance in predicting growth (Fig 4).

Hence this model was later selected in order to safely predict the growth of *E. coli* pD454-MBPeGFP in the whey by-product.

To further validate the effectiveness of the model (Eq. 19) in a food matrix, whey was chosen as a challenging by-product, and the B_f and A_f were estimated. The results of B_f and A_f (0.73 and 1.62, respectively) showed that the model required an adjustment factor to account for the nutrient differences when compared with the culture media system. The modification involves the addition of a correction factor concerning the nutritious differences of the media. Therefore, a *i* correction factor is introduced into Equation 19, which could regulate the growth prediction. The experimental values of the whey-ampicillin-IPTG and the predicted values (Eq. 19) were compared, and based on their difference and application of the correction factor, *i* resulted in being 0.18. The performance of the whey models can be explained in Fig 6, in which the growth prediction capacity of each model is presented. And it is clear that the model Eq. (19), with the addition of the correction factor i = 0.18, predicts more accurately the growth of *E. coli* pD454-MBPeGFP in the whey by-product. The B_f and A_f were re-evaluated and found to be 0.93 and 1.37.

Discussion

The tolerance of *Escherichia coli* pathogenic or non-strains to pathogen interventions such as heat, pressure, and low pH differs substantially among strains. As a result, food manufacturers often apply multiple processes, such as high pressure and MAP, and preservatives, such as acids and salts, to their products to inactivate *Escherichia* contamination (Reineke et al., 2015). Thus, performing challenge tests to study the growth kinetics of *Escherichia* in response to environmental stresses is essential, particularly for developing models for use in predictive microbiology. This study demonstrates the potential of fluorescence as a rapid alternative technique for measuring microbial growth rates in culture medium and by-product matrices and developing predictive models under different temperatures and carbon dioxide-induced climatic stress conditions.

In this study, *E. coli* BL21 (DE3) strain was transformed with the pD454-MBP plasmid, creating an eGFP-tagged strain capable of light emission during growth. Analysis of growth characteristics showed an increase in the lag phase of the *E. coli* pD454-MBPeGFP. This phenomenon was expected, as a 5839 bp increase in genetic material to be replicated should consume a higher level of cellular energy and time for DNA replication, proofreading, and division (Kim et al., 2020). Moreover, the reduction of microbial growth due to the addition of the GFP tags has been studied in different

strains such as *E. coli*, *Pseudomonas putida* and *Streptococcus gordonii* (Sternberg et al., 1999, Hansen et al., 2001). Albeit differences may be minor in one doubling time cycle, slight variation would accumulate over time. However, *E. coli* BL21 (DE3) initially had 4,557,508 bp to start with (Jeong et al., 2009); thus, an approximately 0.13% increase in genomic data might not demonstrate visible differences. Results showed that the plasmid was stable and could be used for monitoring bacterial growth over time.

This study then successfully optimised a fluorescent system for determining the microbial growth of *E. coli* pD454-MBPeGFP in culture media and food by-product by testing different gains. A similar approach was used in the study of Richards et al. (2021), in which a method was optimised by applying death kinetics with fluorescence measurements using SYTOX dye. The authors have tested different gains ranging from 90 to 170 based on the concentration of the dye, the maximum fluorescence signal that the plate reader could detect and the best combination of reproducibility with less background noise. Previous studies have demonstrated the effectiveness of fluorescence for detecting microbial growth, such as the growth of *Acinetobacter johnsonii* in domestic wastewater sludge samples (Rossetti et al., 2007). Similarly, the bioluminescence or fluorescence technology was used by Nyhan et al. (2020) and Krishnamurthi et al. (2021) as an alternative method to determine the μ_{max} of *Listeria* spp. and *E*. *coli* K-12 (MG1655) strain encoding the GFP protein, respectively. They concluded that this method was more rapid and effective than plate counting, while their use is advantageous when other components influence the absorption and scattering in bacterial growth. However, the method had not been used to perform challenge tests in order to determine microbial growth rates.

In this way, the use of alternative and more accurate methods for performing live/dead kinetics assays presents substantial advantages in predictive microbiology. In this study, the combination of fluorescence readings with the g_{time} methodology provided an efficient method for evaluating the μ_{max} of *E. coli* in culture media and food by-products under environmentally stressed conditions. The study of Larentis et al. (2014) evaluated the effect of temperature and IPTG concentration on the expression of a leptospiral protein in *E. coli.* The authors found that *E. coli* grew faster in the highest temperature, 37°C, with μ_{max} equal to 1.05 h^{-1} than at 28°C; however, in our study, the μ_{max} under the same condition was found to be slightly lower, 0.99 h^{-1}. This difference might occur due to the different sizes of the plasmid. Another study by López et al. (2021) used the *E. coli* BL21(DE3) strain and estimated the μ_{max} at three different temperatures of 5, 15, and 25°C in LB. They concluded that

increasing the temperature, increased the μ_{max} to a maximum level of 0.16 h^{-1} at 25°C, which is lower by 0.12 h^{-1} than the μ_{max} reported in this study at 27°C, *i.e.* 0.28 h^{-1}. This difference might occur due to the addition of the plasmid in this study but need to be further evaluated statistically by accounting for the variations between different studies. Finally, bacterial growth reduced as temperature decreased, which is consistent with the results obtained at the concentration of CO_2 0.2% v/v in this study.

However, this study tested different CO_2 levels and concluded that the μ_{max} reached the maximum values under high temperatures with low levels of CO_2 and at low temperatures with high levels of CO_2. However, the latter μ_{max} is significantly lower than the first combination. Couvert et al. (2017) also observed this type of correlation, which concluded that the μ_{max} of *L. monocytogenes* in Brain Heart Infusion broth decreased by 1.14 h^{-1} as the temperature increased from 8 to 37°C, and CO_2 increased from 0.1 to 1% v/v, respectively. Furthermore, Tan and Ng (2020) found that RuBisCo-equipped *E. coli* BL21(DE3) biomass production in LB broth at 37°C was higher by 0.30 g L^{-1} while increasing the levels of CO_2 from 1 to 5% v/v. This behaviour supports the results obtained in the current study, where the growth of *E. coli* at 37°C and 5% v/v CO_2 gave a higher μ_{max}, *i.e.,* 0.31 h^{-1}, than at lower CO_2 levels.

Furthermore, this study developed a method to estimate the DCO_2 in aqueous solutions. In this study, the solubility of CO_2 in LB broth was 0.12 mg L^{-1} at 30°C. In contrast, in the study of Takahashi and Aoyagi (2020), which used LB broth with 5 g L^{-1} NaCl, the solubility was estimated at 0.60 mg L^{-1}. The different concentrations of NaCl in the medium can explain such variation considering that the increase in the salinity of the solution leads to a decrease in the solubility of CO_2 (Belgodere et al., 2015). Furthermore, the pH reduction in the whey-ampicillin-IPTG sample in this study from 6.98 to 5.74 agreed with the results obtained in the study of Lee and Ko (2014). They used whey protein in a MAP with 100% v/v CO_2 stored at room temperature, and the pH of the product was reduced from 7 to 5.70.

To our knowledge, this is the first study on the development of a predictive model for the growth of *E. coli* using the climatic parameters of temperature and DCO_2. According to the findings, the μ_{max} has a maximum at high temperatures with low CO_2 levels, which results in μ_{max} 1.25 h^{-1}. However, some limitations were observed with the developed model, which tends to overestimate the μ_{max} of the bacteria with B_f above 1.00. Sutherland et al. (1997) estimated the μ_{max} of four *E. coli* strains

(NCTC 12079, 204P, W2-2, and 505B) in Tryptone soya broth under MAP conditions by using a polynomial model. They concluded that *E. coli* was relatively resistant to high CO_2 concentrations of 80 and 100% v/v at a temperature of 25°C; this supports the results of the current work in which the μ_{max} at 27°C increased as the CO_2 increased. Another type of secondary model to describe the effect of temperature and % v/v CO_2 was used in the study of Yin et al. (2018). They used the squared root model to predict the μ_{max} of *L. monocytogenes* CICC 21662 in iceberg lettuce packed in MAP conditions. At 10% v/v CO_2, the μ_{max} increased from 0.17 to 0.34 h^{-1} as the temperature increased from 24 to 32°C, which is consistent with the results estimated in the current study under the same conditions. However, the reverse phenomenon was observed at CO_2 concentrations above 20% v/v at the same temperature.

In predictive microbiology, correction factors can typically be added to the model to improve their performance in food matrices (Jay et al., 2007). For that reason, in this study, a correction factor was introduced to improve the predictions of the growth rate of *E. coli* in the whey by-product. The estimated μ_{max} of the whey model after the addition of *i* factor was 0.40 h^{-1} at 37°C and pH of 4.6. This value agrees with the results obtained in the study of Xiong et al. (2020), which found that the μ_{max} of the *E. coli* K12 strain was 0.50 h^{-1} in a bovine whey sample under the same conditions. The difference of 0.10 h^{-1} between the growth rates is expected since the whey model in this study underestimated the rates. Another study by Rosales-Colunga et al. (2010) estimated the growth of *E. coli* W3110 *ΔhycA ΔlacI* strain in whey and found that the growth rate was 1.30 h^{-1} at 37°C and pH 6.5. This result is slightly higher than the value estimation in this study which was 1.28 h^{-1}, which could be explained because of the absence of *hycA* and *lacI* genes in the first case study leading to a reduction in bacterial growth. Additionally, these pH values were not assessed in the current research because they exceed climate change forecasts and the ranges in which our system can operate.

Based on the projections for 2040, it is clear that the increase of the global temperature and atmospheric CO_2 by 1.5°C and 50 ppm, respectively (IPCC, 2019, IPCC, 2018), could increase the growth of *E. coli* which could be present in dairy effluents. Under different environmental stress conditions, the developed polynomial model predicts the growth of *E. coli* pD454-MBPeGFP well in a culture medium and food waste products which could be discarded into the environment. In conclusion, the application of this developed model can be considered a useful tool for predicting the growth of *E. coli* using climate projections. Differences in μ_{max} in relation to elevated climatic

temperatures have been reported for distinct bacteria strains, *i.e.*, *L. monocytogenes, Salmonella enterica, Geobacillus stearothermophilus, Clostridium perfringens, and Bacillus cereus* (Misiou et al., 2021). Testing the model validity under a broader range of media and microbes will help us to better understand the impact of climate change on microorganisms of interest in the food industry.

Acknowledgement

This work was supported by the European Union's Horizon 2020 research and innovation program under the Marie Skłodowska-Curie grant agreement No 813329 (http://www.protect-itn.eu/) (PROTECT).

Declaration of Competing Interest

The authors declare that they have no known competing financial interests or personal relationships that could have appeared to influence the work reported in this paper.

Author Contribution Statement

Styliani Roufou: Conceptualization, Writing – original draft, Methodology, Validation, Formal analysis, Software, Investigation.

Sholeem Griffin: Conceptualization, Validation, Supervision, Writing – review & editing.

Juan Attard: Conceptualization, Validation, Writing – review & editing.

Lydia Katsini: Writing – review & editing.

Monika Polańska: Writing – review & editing.

Jan F.M. Van Impe: Writing – review & editing, Funding acquisition.

Ruben Gatt: Conceptualization, Methodology, Validation, Formal analysis, Supervision, Investigation.

Vasilis P. Valdramidis: Conceptualization, Writing – review & editing, Validation, Supervision, Project administration, Funding acquisition.

Data Availability Statement

Data presented in this manuscript are not available.

References

ADNAN, A. I., ONG, M. Y., NOMANBHAY, S. & SHOW, P. L. 2020. Determination of Dissolved CO2 Concentration in Culture Media: Evaluation of pH Value and Mathematical Data. 8**,** 1373.

AKHLAGHI, Y. G., MA, X., ZHAO, X., SHITTU, S. & LI, J. 2019. A statistical model for dew point air cooler based on the multiple polynomial regression approach. *Energy,* 181**,** 868-881.

ARCARI, T., FEGER, M. L., GUERREIRO, D. N., WU, J. & O'BYRNE, C. P. 2020. Comparative Review of the Responses of Listeria monocytogenes and *Escherichia coli* to Low pH Stress. *Genes (Basel),* 11.

BAG, M. A. S., KHAN, M. S. R., SAMI, M. D. H., BEGUM, F., ISLAM, M. S., RAHMAN, M. M., RAHMAN, M. T. & HASSAN, J. 2021. Virulence determinants and antimicrobial resistance of *E. coli* isolated from bovine clinical mastitis in some selected dairy farms of Bangladesh. *Saudi Journal of Biological Sciences,* 28**,** 6317-6323.

BELGODERE, C., DUBESSY, J., VAUTRIN, D., CAUMON, M.-C., STERPENICH, J., PIRONON, J., ROBERT, P., RANDI, A. & BIRAT, J.-P. 2015. Experimental determination of CO2 diffusion coefficient in aqueous solutions under pressure at room temperature via Raman spectroscopy: impact of salinity (NaCl). 46**,** 1025-1032.

BEVINGTON, P. R. & ROBINSON, D. K. 2003. Error Propagation. *In:* HILL, M. G. (ed.) *Data Reduction and Error Analysis for the Physical Sciences.* 3rd ed.: Kent A. Peterson.

BOZ, Z., WELT, B. A., BRECHT, J. K., PELLETIER, W., MCLAMORE, E., KIKER, G. A. & AND BUTLER, J. E. 2018. Review of Challenges and Advances in Modification of Food Package Headspace Gases. *Journal of Applied Packaging Research* [Online], 10. Available: https://scholarworks.rit.edu/japr/vol10/iss1/5 [Accessed 06 Apr 2018].

COUVERT, O., GUÉGAN, S., HÉZARD, B., HUCHET, V., LINTZ, A., THUAULT, D. & STAHL, V. 2017. Modeling carbon dioxide effect in a controlled atmosphere and its interactions with temperature and pH on the growth of *L. monocytogenes* and *P. fluorescens*. *Food Microbiology,* 68**,** 89-96.

CUPPERS, H. G. A. M. & SMELT, J. P. P. M. 1993. Time to turbidity measurement as a tool for modeling spoilage by *Lactobacillus*. *Journal of Industrial Microbiology,* 12**,** 168-171.

DA SILVA DUARTE, V., CARLOT, M., PAKROO, S., TARRAH, A., LOMBARDI, A., SANTIAGO, H., CORICH, V. & GIACOMINI, A. 2020. Comparative evaluation of cheese whey microbial composition from four Italian cheese factories by viable counts and 16S rRNA gene amplicon sequencing. *International Dairy Journal,* 104**,** 104656.

DTE, S. 2021. *Atmospheric CO2 levels may rise 50% higher than pre-industrial levels: Recent estimates* [Online]. Available: https://www.downtoearth.org.in/news/climate-change/atmospheric-co2-levels-may-rise-50-higher-than-pre-industrial-levels-recent-estimates-75992#:~:text=The%20annual%20average%20CO2%20concentration%20for%202021%20could%20be%20around,industrial%20levels%2C%20the%20estimates%20noted. [Accessed 17 March 2021 2021].

ENGELBRECHT, C. J., GÖBEL, W. & HELMCHEN, F. 2009. Enhanced fluorescence signal in nonlinear microscopy through supplementary fibre-optic light collection. *Optics Express,* 17**,** 6421-6435.

GANINI, D., LEINISCH, F., KUMAR, A., JIANG, J., TOKAR, E. J., MALONE, C. C., PETROVICH, R. M. & MASON, R. P. 2017. Fluorescent proteins such as eGFP lead to catalytic oxidative stress in cells. *Redox Biol,* 12**,** 462-468.

GLEN, S. 2021. *F Statistic / F Value: Simple Definition and Interpretation"* [Online]. StatisticsHowTo.com. Available: https://www.statisticshowto.com/probability-and-statistics/f-statistic-value-test/ [Accessed 23/02/2022].

654 GOMES, L., MONTEIRO, G. & MERGULHÃO, F. 2020. The Impact of IPTG Induction on Plasmid
655 Stability and Heterologous Protein Expression by *Escherichia coli* Biofilms. *Int J Mol Sci,* 21.
656 HANSEN, M. C., PALMER, R. J., UDSEN, C., WHITE, D. C. & MOLIN, S. 2001. Assessment of GFP
657 fluorescence in cells of *Streptococcus gordonii* under conditions of low pH and low oxygen
658 concentration. 147**,** 1383-1391.
659 HELD, P. 2018. *Using Phenol Red to Assess pH in Tissue Culture Media* [Online]. USA: BioTek
660 Instruments. Available: https://www.biotek.com/resources/application-notes/using-
661 phenol-red-to-assess-ph-in-tissue-culture-media/ [Accessed March 22, 2018 2018].
662 HUANG, Y., LIU, X., LAWS, E. A., CHEN, B., LI, Y., XIE, Y., WU, Y., GAO, K. & HUANG, B. 2018. Effects
663 of increasing atmospheric CO(2) on the marine phytoplankton and bacterial metabolism
664 during a bloom: A coastal mesocosm study. *Sci Total Environ,* 633**,** 618-629.
665 IPCC 2018. TAR Climate Change 2001: The Scientific Basis, The Carbon Cycle and Atmospheric
666 Carbon Dioxide [G.D. Farquhar, M.J.R. Fasham, M.L. Goulden, M. Heimann, V.J. Jaramillo,
667 H.S. Kheshgi, C. Le Quéré,R.J. Scholes, D.W.R. Wallace]. *In:* IPCC (ed.).
668 IPCC 2019. Climate Change and Land: an IPCC special report on climate change, desertication, land
669 degradation, sustainable land management, food security, and greenhouse gas uxes in
670 terrestrial ecosystems [P.R. Shukla, J. Skea, E. Calvo Buendia, V. Masson-Delmotte, H.-O.
671 Pörtner, D.C. Roberts, P. Zhai, R. Slade, S. Connors, R. van Diemen, M. Ferrat, E. Haughey, S.
672 Luz, S. Neogi, M. Pathak, J. Petzold, J. Portugal Pereira, P. Vyas, E. Huntley, K. Kissick, M.
673 Belkacemi, J. Malley, (eds.)]. *In:* IPCC (ed.).
674 JAY, O., REARDON, F. D., WEBB, P., DUCHARME, M. B., RAMSAY, T., NETTLEFOLD, L. & KENNY, G. P.
675 2007. Estimating changes in mean body temperature for humans during exercise using core
676 and skin temperatures is inaccurate even with a correction factor. 103**,** 443-451.
677 JEONG, H., BARBE, V., LEE, C. H., VALLENET, D., YU, D. S., CHOI, S. H., COULOUX, A., LEE, S. W., YOON,
678 S. H., CATTOLICO, L., HUR, C. G., PARK, H. S., SÉGURENS, B., KIM, S. C., OH, T. K., LENSKI, R.
679 E., STUDIER, F. W., DAEGELEN, P. & KIM, J. F. 2009. Genome sequences of *Escherichia coli* B
680 strains REL606 and BL21(DE3). *J Mol Biol,* 394**,** 644-52.
681 KANDA, T., ABIKO, G., KANESAKI, Y., YOSHIKAWA, H., IWAI, N. & WACHI, M. 2020. RNase E-
682 dependent degradation of tnaA mRNA encoding tryptophanase is prerequisite for the
683 induction of acid resistance in *Escherichia coli*. *Scientific Reports,* 10**,** 7128.
684 KIM, J., DARLINGTON, A., SALVADOR, M., UTRILLA, J. & JIMÉNEZ, J. I. 2020. Trade-offs between gene
685 expression, growth and phenotypic diversity in microbial populations. *Current Opinion in*
686 *Biotechnology,* 62**,** 29-37.
687 KOUTSOUMANIS, K. P. & SOFOS, J. N. 2004. Comparative acid stress response of Listeria
688 monocytogenes, *Escherichia coli* O157:H7 and Salmonella Typhimurium after habituation at
689 different pH conditions. *Letters in Applied Microbiology,* 38**,** 321-326.
690 KRISHNAMURTHI, V. R., NIYONSHUTI, I. I., CHEN, J. & WANG, Y. 2021. A new analysis method for
691 evaluating bacterial growth with microplate readers. *PLOS ONE,* 16**,** e0245205.
692 KRUYER, N. S. & PERALTA-YAHYA, P. 2020. Advancing the Potential for the Production of Chemicals
693 from Carbon Dioxide in *Escherichia coli*. *Biochemistry,* 59**,** 731-732.
694 LAI, C.-Z., DEGRANDPRE, M. D., WASSER, B. D., BRANDON, T. A., CLUCAS, D. S., JAQUETH, E. J.,
695 BENSON, Z. D., BEATTY, C. M. & SPAULDING, R. S. 2016. Spectrophotometric measurement
696 of freshwater pH with purified meta-cresol purple and phenol red. *Limnology and*
697 *Oceanography: Methods,* 14**,** 864-873.
698 LARENTIS, A. L., NICOLAU, J. F. M. Q., ESTEVES, G. D. S., VARESCHINI, D. T., DE ALMEIDA, F. V. R.,
699 DOS REIS, M. G., GALLER, R. & MEDEIROS, M. A. 2014. Evaluation of pre-induction
700 temperature, cell growth at induction and IPTG concentration on the expression of a
701 leptospiral protein in *E. coli* using shaking flasks and microbioreactor. *BMC Research Notes,*
702 7**,** 671.

LEE, K. & KO, S. 2014. Proof-of-concept study of a whey protein isolate based carbon dioxide indicator to measure the shelf-life of packaged foods. *Food Science and Biotechnology,* 23**,** 115-120.

LÓPEZ, A. L. M., ACOSTA-GONZÁLEZ, A., MANRIQUE, I. Y. P., CORREA, R. E. P. & JUNCA, C. J. 2021. Optimization of Fermentation Conditions for Recombinant Lipase Expression At Small Scale Using Response Surface Methodology for Preliminary Production In Two Bioreactor Platforms. *Research Square*.

LOWDER, M., UNGE, A., MARAHA, N., JANSSON, J. K., SWIGGETT, J. & OLIVER, J. D. 2000. Effect of starvation and the viable-but-nonculturable state on green fluorescent protein (GFP) fluorescence in GFP-tagged *Pseudomonas* fluorescens A506. *Appl Environ Microbiol,* 66**,** 3160-5.

MEMBRE, J. M., LEPORQ, B., VIALETTE, M., METTLER, E., PERRIER, L. & & ZWIETERING, M. H. 2002. Experimental protocols and strain variability of cardinal values (pH and Aw) of bacteria using Bioscreen C : microbial and statistical aspects. *In:* AXELSSON L, T. E., MEROK KJ, (ed.) *Food Micro 2002: Microbial adaptation to changing environments : 18th Symposium of the International Committee on Food Microbiology and Hygiene.* Lillehammer, Norway, 2002. As, Norway: Matforsk. 2002.

MERLIN, C., MASTERS, M., MCATEER, S. & COULSON, A. 2003. Why Is Carbonic Anhydrase Essential to *Escherichia coli*. *Journal of Bacteriology,* 185**,** 6415.

MILLERO, F. J., GRAHAM, T. B., HUANG, F., BUSTOS-SERRANO, H. & PIERROT, D. 2006. Dissociation constants of carbonic acid in seawater as a function of salinity and temperature. *Marine Chemistry,* 100**,** 80-94.

MIRAGLIA, M., MARVIN, H. J. P., KLETER, G. A., BATTILANI, P., BRERA, C., CONI, E., CUBADDA, F., CROCI, L., DE SANTIS, B., DEKKERS, S., FILIPPI, L., HUTJES, R. W. A., NOORDAM, M. Y., PISANTE, M., PIVA, G., PRANDINI, A., TOTI, L., VAN DEN BORN, G. J. & VESPERMANN, A. 2009. Climate change and food safety: An emerging issue with special focus on Europe. *Food and Chemical Toxicology,* 47**,** 1009-1021.

MISIOU, O., KASIOURAS, G. & KOUTSOUMANIS, K. 2021. Development and validation of an extended predictive model for the effect of pH and water activity on the growth kinetics of *Geobacillus stearothermophilus* in plant-based milk alternatives. *Food Research International,* 145**,** 110407.

NYHAN, L., BEGLEY, M., JOHNSON, N. & CALLANAN, M. 2020. An evaluation of Lux technology as an alternative methodology to determine growth rates of *Listeria* in laboratory media and complex food matrices. *International Journal of Food Microbiology,* 317**,** 108442.

OLIVEIRA, M., USALL, J., SOLSONA, C., ALEGRE, I., VIÑAS, I. & ABADIAS, M. 2010. Effects of packaging type and storage temperature on the growth of foodborne pathogens on shredded 'Romaine' lettuce. *Food Microbiology,* 27**,** 375-380.

RAJAPAKSHA, P., ELBOURNE, A., GANGADOO, S., BROWN, R., COZZOLINO, D. & CHAPMAN, J. 2019. A review of methods for the detection of pathogenic microorganisms. *Analyst,* 144**,** 396-411.

REINEKE, K., SEVENICH, R., HERTWIG, C., JANßEN, T., FRÖHLING, A., KNORR, D., WIELER, L. H. & SCHLÜTER, O. 2015. Comparative study on the high pressure inactivation behavior of the Shiga toxin-producing *Escherichia coli* O104:H4 and O157:H7 outbreak strains and a non-pathogenic surrogate. *Food Microbiology,* 46**,** 184-194.

RICHARDS, R., HONEYWELL, M. E. & LEE, M. J. 2021. FLICK: An optimized plate reader-based assay to infer cell death kinetics. *STAR Protocols,* 2**,** 100327.

ROSALES-COLUNGA, L. M., RAZO-FLORES, E., ORDOÑEZ, L. G., ALATRISTE-MONDRAGÓN, F. & DE LEÓN-RODRÍGUEZ, A. 2010. Hydrogen production by *Escherichia coli* Δ*hycA* Δ*lacI* using cheese whey as substrate. *International Journal of Hydrogen Energy,* 35**,** 491-499.

ROSS, T. 1996. Indices for performance evaluation of predictive models in food microbiology. *J Appl Bacteriol,* 81**,** 501-8.

ROSSETTI, S., TOMEI, M. C., BLACKALL, L. L. & TANDOI, V. 2007. Bacterial growth kinetics estimation by fluorescence in situ hybridization and spectrofluorometric quantification. 44**,** 643-648.

ROUFOU, S., GRIFFIN, S., KATSINI, L., POLAŃSKA, M., VAN IMPE, J. F. M. & VALDRAMIDIS, V. P. 2021. The (potential) impact of seasonality and climate change on the physicochemical and microbial properties of dairy waste and its management. *Trends in Food Science & Technology,* 116**,** 1-10.

ROUFOU, S., GRIFFIN, S., OLIVEIRA MALLIA, J., KATSINI, L., POLAŃSKA, M., VAN IMPE, J. F. M., GATT, R. & VALDRAMIDIS, V. P. 2022. Towards a novel quantitative method for determination of pH and dissolved CO2 concentration in different culture media. *FoodSim2022.* Ghent, Belgium: EUROSIS-ETI

SHARMA, M., LAKSHMAN, S., FERGUSON, S., INGRAM, D. T., LUO, Y. & PATEL, J. 2011. Effect of modified atmosphere packaging on the persistence and expression of virulence factors of *Escherichia coli* O157:H7 on shredded iceberg lettuce. *J Food Prot,* 74**,** 718-26.

SONG, Y. S., STEWART, D., REINEKE, K., WANG, L., MA, C., LU, Y., SHAZER, A., DENG, K. & TORTORELLO, M. L. 2019. Effects of Package Atmosphere and Storage Conditions on Minimizing Risk of *Escherichia coli* O157:H7 in Packaged Fresh Baby Spinach. *Journal of Food Protection,* 82**,** 844-853.

STERNBERG, C., CHRISTENSEN BJARKE, B., JOHANSEN, T., TOFTGAARD NIELSEN, A., ANDERSEN JENS, B., GIVSKOV, M. & MOLIN, S. 1999. Distribution of Bacterial Growth Activity in Flow-Chamber Biofilms. *Applied and Environmental Microbiology,* 65**,** 4108-4117.

STUMM, W. & MORGAN, J. J. 1996. Aquatic Chemistry : Chemical Equilibria and Rates in Natural Waters. 3rd ed. ed.: New York : Wiley.

SUTHERLAND, J. P., BAYLISS, A. J., BRAXTON, D. S. & BEAUMONT, A. L. 1997. Predictive modelling of *Escherichia coli* O157:H7: Inclusion of carbon dioxide as a fourth factor in a pre-existing model. *International Journal of Food Microbiology,* 37**,** 113-120.

TAKAHASHI, M. & AOYAGI, H. 2020. Analysis and effect of conventional flasks in shaking culture of *Escherichia coli*. *AMB Express,* 10**,** 77.

TAN, S.-I. & NG, I. S. 2020. Design and optimization of bioreactor to boost carbon dioxide assimilation in RuBisCo-equipped *Escherichia coli*. *Bioresource Technology,* 314**,** 123785.

TASHIRO, Y., HIRANO, S., MATSON, M. M., ATSUMI, S. & KONDO, A. 2018. Electrical-biological hybrid system for CO(2) reduction. *Metab Eng,* 47**,** 211-218.

VALDRAMIDIS, V. P., CULLEN, P. J., TIWARI, B. K. & O'DONNELL, C. P. 2010. Quantitative modelling approaches for ascorbic acid degradation and non-enzymatic browning of orange juice during ultrasound processing. *Journal of Food Engineering,* 96**,** 449-454.

WANG, X., ZORRAQUINO, V., KIM, M., TSOUKALAS, A. & TAGKOPOULOS, I. 2018. Predicting the evolution of *Escherichia coli* by a data-driven approach. *Nature Communications,* 9**,** 3562.

XIONG, L., LI, C., BOEREN, S., VERVOORT, J. & HETTINGA, K. 2020. Effect of heat treatment on bacteriostatic activity and protein profile of bovine whey proteins. *Food Research International,* 127**,** 108688.

YADAV, J. S. S., YAN, S., PILLI, S., KUMAR, L., TYAGI, R. D. & SURAMPALLI, R. Y. 2015. Cheese whey: A potential resource to transform into bioprotein, functional/nutritional proteins and bioactive peptides. *Biotechnology Advances,* 33**,** 756-774.

YAO, W. & BYRNE, R. H. 2001. Spectrophotometric determination of freshwater pH using bromocresol purple and phenol red. *Environ Sci Technol,* 35**,** 1197-201.

YIN, X., ZHANG, Y., TU, S., HUANG, Y. & TU, K. 2018. Model for the Effect of Carbon Dioxide on *Listeria Monocytogenes* in Fresh-cut Iceberg Lettuce Packaged Under Modified Atmosphere. *Food Science and Technology Research,* 24**,** 1021-1027.

ZHANG, J., QIONG;, L., CHEN YU-MIAO, LIU ZHAO-QING & CHANG-WEI, X. 2012. Determination of Acid Dissociation Constant of Methyl Red by Multi-Peaks Gaussian Fitting Method Based on UV-Visible Absorption Spectrum. 28**,** 1030-1036.

ZHU, L.-W., ZHANG, L., WEI, L.-N., LI, H.-M., YUAN, Z.-P., CHEN, T., TANG, Y.-L., LIANG, X.-H. & TANG, Y.-J. 2015. Collaborative regulation of CO2 transport and fixation during succinate production in *Escherichia coli*. *Scientific Reports,* 5**,** 17321.

Tables

Table 1. Results of the secondary fitted model Equation (12) parameter estimates when applying the *partial F-test* (parameters which supported the Null Hypothesis marked in bold).

Parameters	Estimated values	Standard Error	Partial F-test
b_0	-8.23	1.14	46.87
b_1	0.42	0.07	39.49
b_2	0.01	8.80×10^{-4}	68.67
b_3	-2.77×10^{-4}	2.50×10^{-5}	113.57
b_4	-4.56×10^{-3}	9.00×10^{-4}	23.51
b_5	**1.30×10^{-7}**	**7.08×10^{-7}**	**2.04**

Table 2. Results of the secondary fitted model Equation (13) parameter estimates when applying the *partial F-test* (parameters which supported the Null Hypothesis marked in bold).

Parameters	Estimated values	Standard Error	Partial F-test
b_0	29.40	8.31	10.04
b_1	-2.87	0.73	12.47
b_2	4.72×10^{-3}	4.18×10^{-4}	4.91
b_3	0.09	0.02	14.70
b_4	**-2.07×10^{-5}**	**4.06×10^{-6}**	**0.12**
b_5	-3.91×10^{-6}	3.27×10^{-7}	5.43
b_6	**4.48×10^{-7}**	**9.43×10^{-8}**	**0.98**
b_7	-9.00×10^{-4}	2.03×10^{-4}	15.97
b_8	**3.59×10^{-9}**	**9.79×10^{-10}**	**3.60**

Figures

816

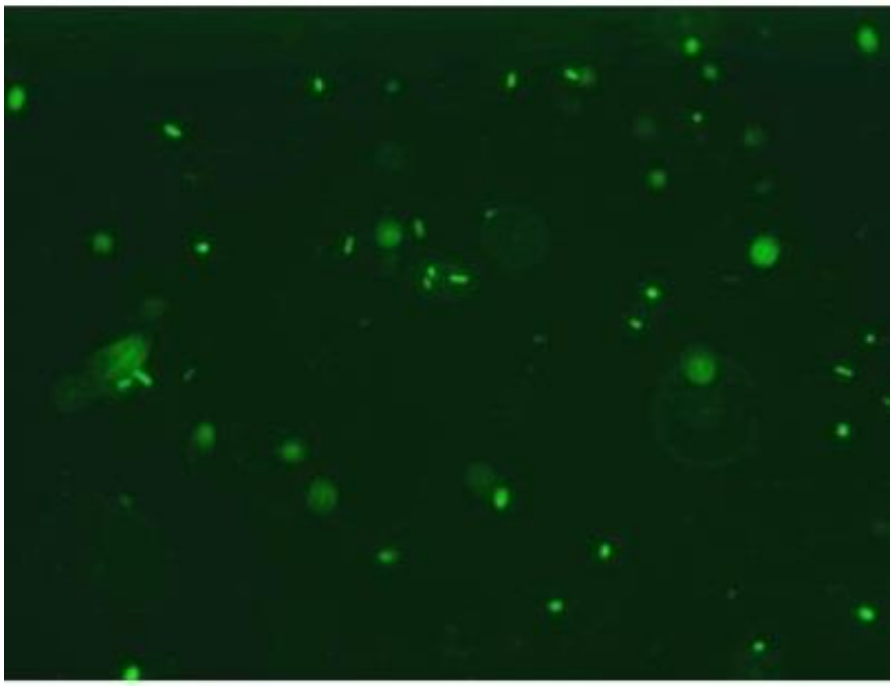

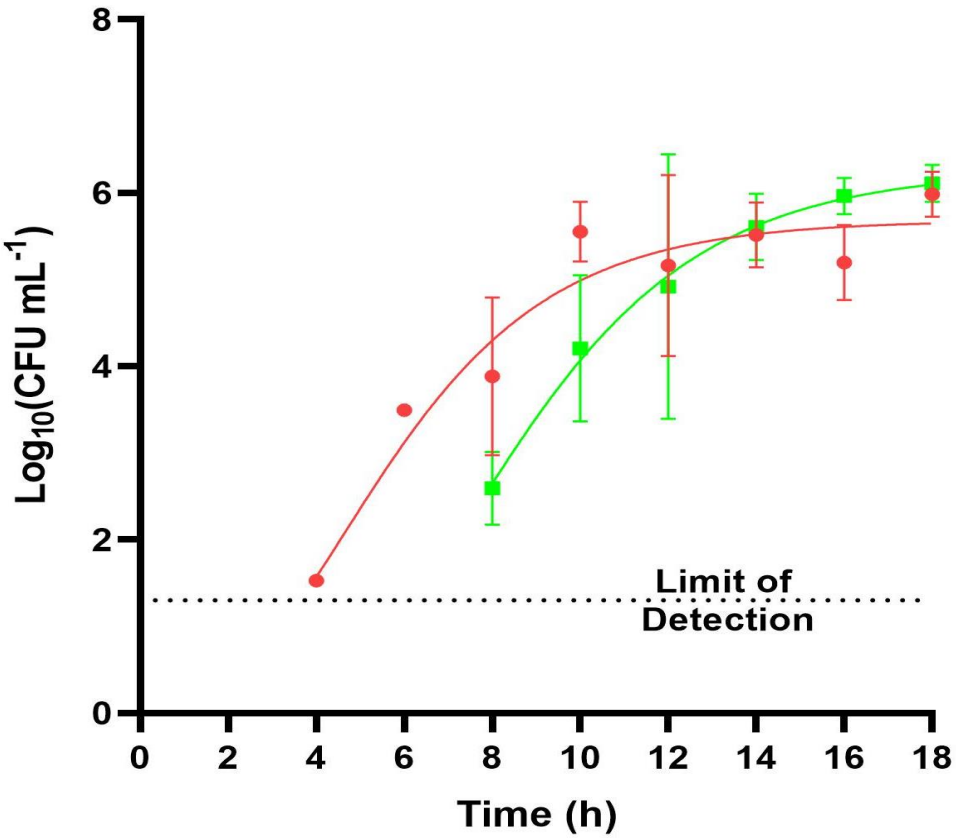

817

818 **Figure 1. a**: Staining and fluorescent imaging validated *E. coli* BL21 (DE3) pD454-MBPeGFP growth
819 after 24h at 37°C, **b**: Growth of *E. coli* BL21 (DE3) (▪) and *E. coli* BL21 (DE3) pD454-MBPeGFP (●), at
820 37°C generated by viable plate counts.

821

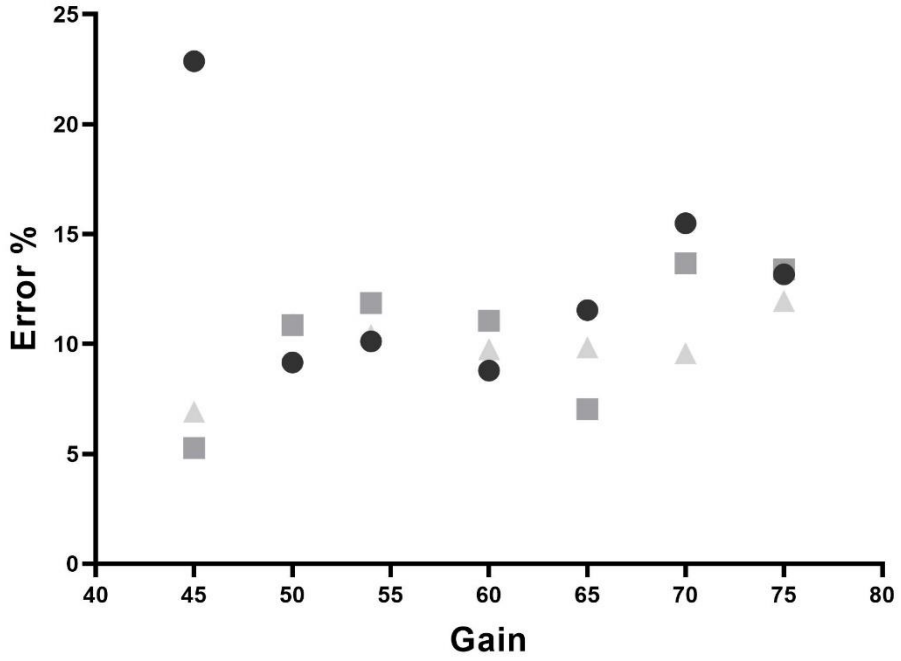

822

823 **Figure 2.** The percentage error of the gains at different inoculum sizes (● 10,000 CFU mL^{-1}, ▪ 100,000

824 CFU mL^{-1}, ▲ 1,000,000 CFU mL^{-1}) in LB-ampicillin-IPTG broth.

825

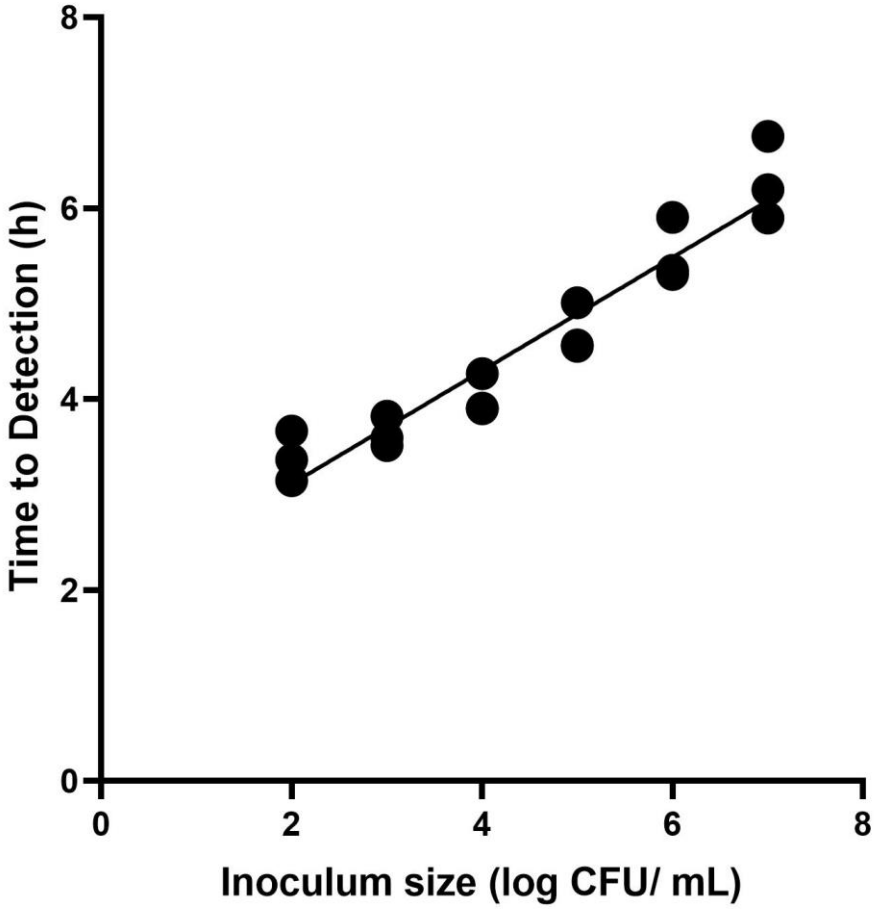

826

Figure 3. Illustration of calculating the specific growth rate (μ_{max}) from three replicates of six binary dilutions (N) at 40°C with 0.2% v/v CO_2 in LB-ampicillin-IPTG broth (R^2= 0.92).

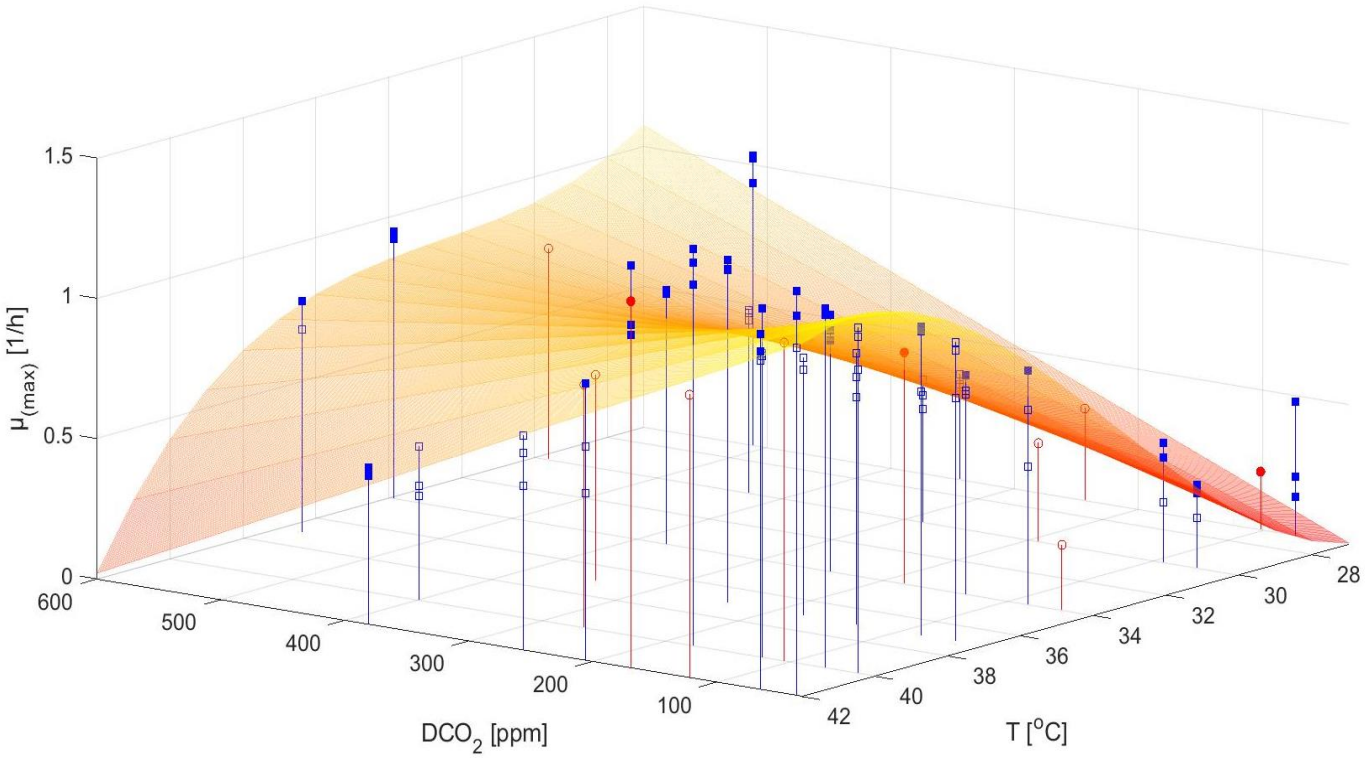

Figure 4. The experimental (□) and predicted specific growth rates of *E. coli* pD454-MBPeGFP in LB broth as a function of temperature and dissolved CO_2 as described by Equation (19). The symbol ° represents the validation dataset. In both datasets, the solid symbols denote data above the predicted specific growth rates.

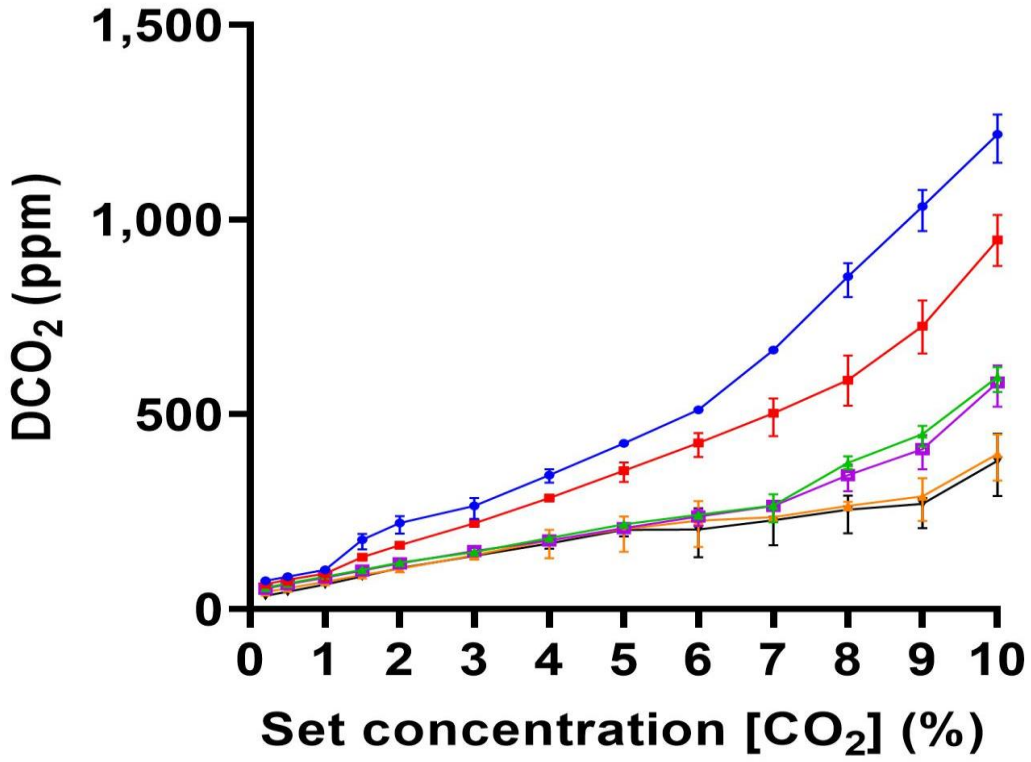
1,500
1,000
500
0
DCO2 (ppm)
0 1 2 3 4 5 6 7 8 9 10
Set concentration [CO2] (%)

836

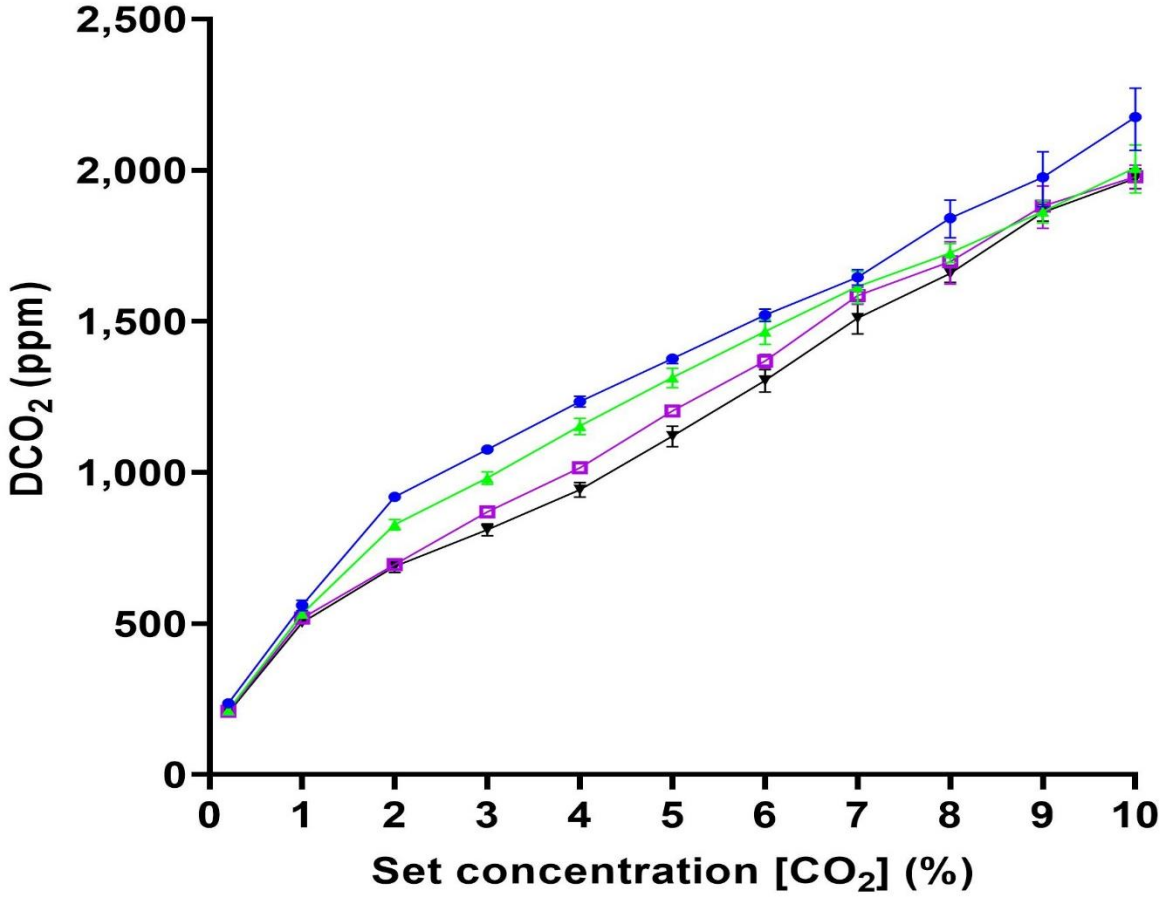
2,500
2,000
1,500
1,000
500
0
DCO2 (ppm)
0 1 2 3 4 5 6 7 8 9 10
Set concentration [CO2] (%)

837

Figure 5. Dissolved CO_2 in nutrient broth as a function of CO_2 in the gas phase and temperature. **a**: LB-ampicillin-IPTG broth (blue ● 27°C, red ▪ 30°C, green ▲ 35°C, purple □ 37°C, orange * 40°C, and black ▼ 42°C), **b**: whey-ampicillin-IPTG sample (blue ● 27°C, green ▲ 35°C, purple □ 37°C, and black ▼ 42°C).

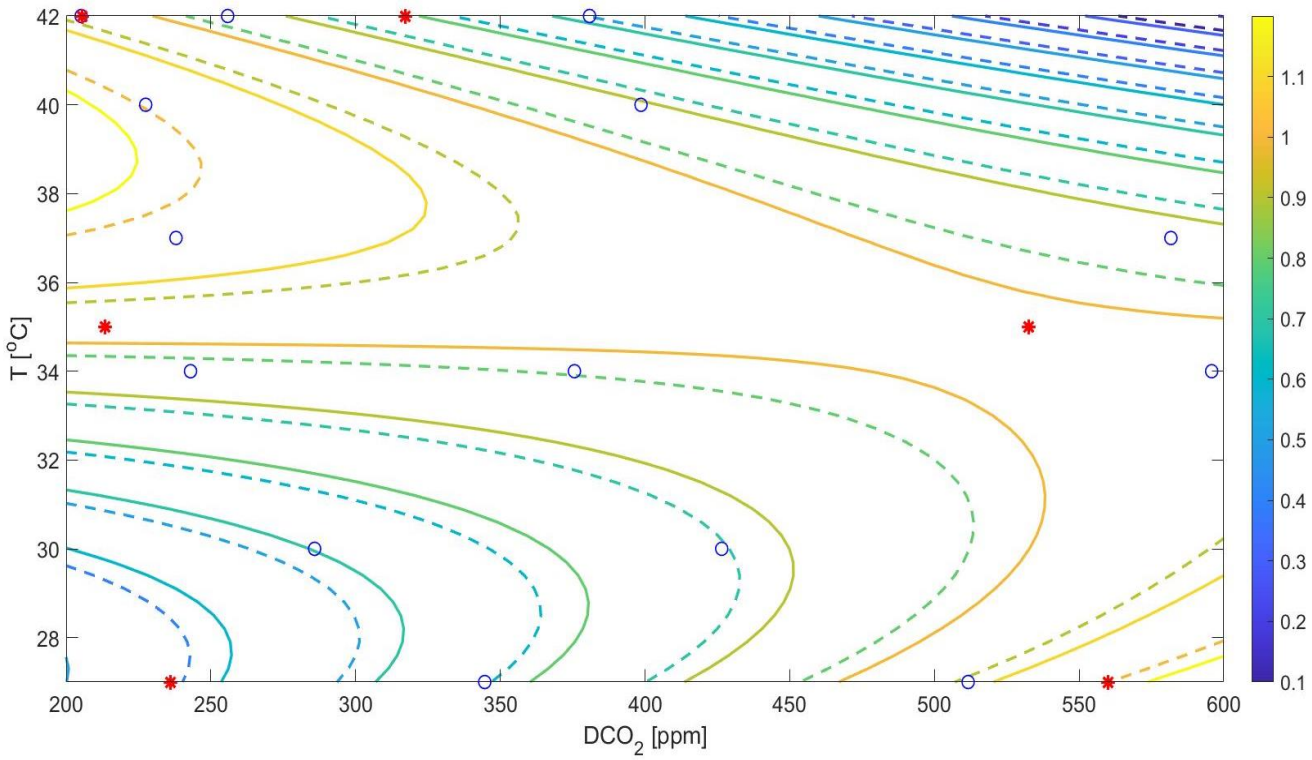

Figure 6. The specific growth rates of *E. coli* pD454-MBPeGFP in whey samples as a function of temperature and dissolved CO_2 as described by Equation (19) (dashed line) and Equation (19) with the addition of the correction factor,*i*, (solid line) are depicted. The * represents the experimental data of the whey dataset, and ° represents the validation dataset of the broth.